

ON CALCULATIONS OF THE DIPOLE MOMENT FROM THE ELECTRON DENSITY DATA

MARIAN GRZYCIUK AND JERZY GÓRECKI

*Institute of Physical Chemistry PAS,
Kasprzaka 44/52, 01-224 Warsaw, Poland
{majgryn, gorecki}@ichf.edu.pl*

(Received 12 August 2002; revised manuscript received 30 August 2002)

Abstract: In the paper we discuss how to calculate the dipole moment using the electron density data. A few numerical methods are compared. We have found that usually the interpolation of electron density gives the most accurate results.

Keywords: electron density, dipole moment, grids

1. Introduction

There are many commercial programs, which allow one to perform the density functional calculations and to find ground states of medium size systems. Programs are, for example, used to estimate the binding energies for molecules adsorbed on surfaces and to find the preferred adsorption sites. Such programs like CASTEP (Accelrys Inc.) [1, 2] give also information on the electron density as a function of space. Therefore, one may use these data and calculate the dipole moment of the system studied. Such information is important because the dipole moment of adsorbed atoms can be measured in experiments [3], for example, using the static capacitor method for measurements of the surface potential of gases adsorbed on evaporated metal films [4]. According to MacDonald and Barlow's the following equation describes the surface potential SP [5]:

$$\text{SP} = 4\pi\mu_0 n_a (1 + 9\alpha n_a^{3/2}) \quad [\text{mV}], \quad (1)$$

where n_a [at/cm²] and α [cm³] denote concentration and polarizability of the adsorbate and μ_0 [D] is the normal component of its dipole moment at $n_a \sim 0$. If the amount of adsorbed substance (for example hydrogen) is low then the surface potential, which can be directly measured, is proportional to n_a and the proportionality constant is related to the dipole moment. It would be interesting to compare such result with numerical calculations.

Figure 1 shows the cluster representing (100) the surface of TiH₂. The cluster consists of 6 atoms of titanium and 8 atoms of hydrogen, because, due to the periodic

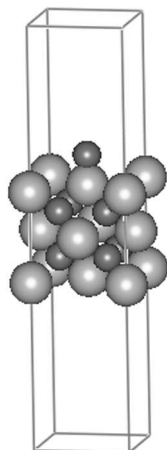


Figure 1. The (100) surface of TiH_2 with adsorbed atoms of hydrogen

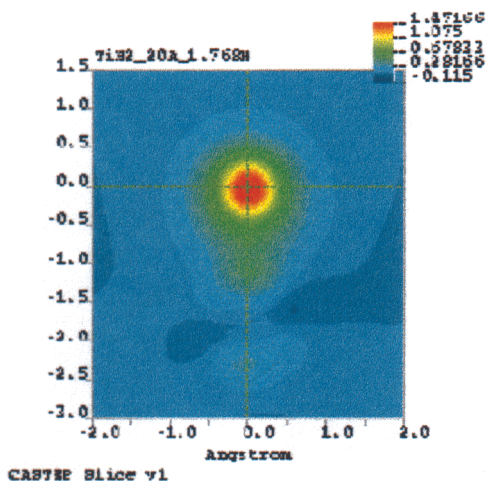


Figure 2. The electron density for atom of hydrogen adsorbed on the (100) surface of TiH_2 in the top position: distances on both axes are given in \AA

boundary conditions, the Ti atoms at the cell's edges belong to the neighbouring cells, too. There is an additional hydrogen atom adsorbed at the top position over the central titanium atom. Figure 2 shows the electron density around the hydrogen atom adsorbed on the (100) surface of TiH_2 in the top position. As one can see, the electron density is not spherically symmetric, so a dipole moment different from zero is expected.

For the periodic boundary conditions used, the cluster represents a two-dimensional layer of TiH_2 . The electron densities for a TiH_2 cluster with and without the hydrogen atom are usually different, so the dipole moments of both systems are different, too. Formally, one may calculate them, subtract one from another and thus obtain the change in the dipole moment of the surface caused by the presence of a single hydrogen atom (or precisely, by a submonolayer of hydrogen). But is such approach accurate enough? The problem is caused by the fact that density functional packages do not give us the functional form of the electron density, but the electron density averaged over a small area of space around the grid points.

2. Theory

The CASTEP program [1, 2] uses the density functional theory to calculate the electron density of the ground state of many atom systems. The functional for the exchange/correlation contribution may be approximated within the local density approximation and the gradient correction may be taken into account. The electron-ion interaction is described using pseudopotential concept. For transition metals the pseudopotential is generated using the optimization scheme of Lin [6]. It is transferable (i.e. can be used in different chemical environments), and sufficiently soft (relatively small basis can be used). The program uses the periodic boundary conditions so it is especially useful in studying the properties of crystalline solids and periodic surfaces.

If a single molecule is studied then the cell should be large enough to avoid interactions with its replicas. CASTEP performs optimization of wavefunctions in reciprocal space. The minimisation is achieved using band-by-band technique. CASTEP uses special k -point sampling for integration over the Brillouin zone, fast Fourier transforms (FFT) to evaluate matrix elements, and wavefunction symmetrization for crystals with point-group symmetry higher than P_1 . The small k -point sampling with a kinetic energy cut-off 400–600 eV was used in calculation. Finally, the program returns the values of electron density at the lattice points inside the simulated cell in the real space. The number of these points is a control parameter of the program and we usually use between 30 and 100 points in each direction. CASTEP includes a procedure based on Gasteiger method [7], which calculates the dipole moment, but as we show below it is not accurate and it is worthwhile to study other approaches.

Let us consider the simulated supercell C in the form:

$$[x_{\min}, x_{\max}] \times [y_{\min}, y_{\max}] \times [z_{\min}, z_{\max}]$$

where x_{\min} , x_{\max} , y_{\min} , y_{\max} , z_{\min} , z_{\max} give the range of grid points. The numbers of grid points in each direction are ii , jj , kk , respectively.

Let $\rho(x, y, z)$ denote the electron density function. The total charge of electrons is:

$$\rho_C = \iiint_C \rho(x, y, z) dv \quad (2)$$

and the dipole moment of the system composed of electrons and atomic cores (nuclei) is:

$$\vec{\mu} = \sum_m \vec{r}_m q_m + \iiint_C \vec{r} \rho(x, y, z) dv, \quad (3)$$

where \vec{r}_m are the positions of the nuclei, and q_m are their charges.

The integrals in Equations (2) and (3) can be evaluated by a number of different methods. In the following we consider a few of them, namely:

1. The direct method:

$$\rho^d = \sum_{i=1}^{ii} \sum_{j=1}^{jj} \sum_{k=1}^{kk} f(i, j, k), \quad \vec{\mu}^d = \sum_{i=1}^{ii} \sum_{j=1}^{jj} \sum_{k=1}^{kk} \vec{r}(i, j, k) \cdot f(i, j, k), \quad (4)$$

where

$$f(i, j, k) = \int_{x_i - \Delta x/2}^{x_i + \Delta x/2} dx \int_{y_j - \Delta y/2}^{y_j + \Delta y/2} dy \int_{z_k - \Delta z/2}^{z_k + \Delta z/2} dz \rho(x, y, z),$$

where $i = 1, \dots, ii$; $j = 1, \dots, jj$; $k = 1, \dots, kk$ and

$$\vec{r}(i, j, k) = \left[x_{\min} + i \cdot \Delta x - \frac{\Delta x}{2}, y_{\min} + j \cdot \Delta y - \frac{\Delta y}{2}, z_{\min} + k \cdot \Delta z - \frac{\Delta z}{2} \right].$$

The values of $f(i, j, k)$ at the grid points correspond to the electron density obtained from CASTEP.

2. The integration by parts:

$$\rho^I = \sum_{i=1}^{ii} \sum_{j=1}^{jj} \sum_{k=1}^{kk} f(i, j, k), \quad \bar{\mu}^I = [\mu_x, \mu_y, \mu_z], \quad (5)$$

where

$$\begin{aligned} \mu_x &= x_{\max} \cdot \rho^I - \int_{x_{\min}}^{x_{\max}} dx \int_{x_{\min}}^x ds \int_{y_{\min}}^{y_{\max}} dy \int_{z_{\min}}^{z_{\max}} dz \rho(s, y, z), \\ \mu_y &= y_{\max} \cdot \rho^I - \int_{y_{\min}}^{y_{\max}} dy \int_{y_{\min}}^y ds \int_{x_{\min}}^{x_{\max}} dx \int_{z_{\min}}^{z_{\max}} dz \rho(x, s, z), \\ \mu_z &= z_{\max} \cdot \rho^I - \int_{z_{\min}}^{z_{\max}} dz \int_{z_{\min}}^z ds \int_{x_{\min}}^{x_{\max}} dx \int_{y_{\min}}^{y_{\max}} dy \rho(x, y, s). \end{aligned}$$

Here the fourth order integrals are evaluated using the simplest step-by-step Euler integration.

3. The Taylor expansion method:

$$\begin{aligned} \rho^{T,n} &= \sum_{i=1}^{ii} \sum_{j=1}^{jj} \sum_{k=1}^{kk} f_T^n(i, j, k), \\ \bar{\mu}^{T,n} &= \sum_{i=1}^{ii} \sum_{j=1}^{jj} \sum_{k=1}^{kk} \vec{r}(i, j, k) \cdot f_T^n(i, j, k), \\ f_T^n(i, j, k) &= \int_{x_i - \Delta x/2}^{x_i + \Delta x/2} dx \int_{y_j - \Delta y/2}^{y_j + \Delta y/2} dy \int_{z_k - \Delta z/2}^{z_k + \Delta z/2} dz f_T^n(i, j, k, x, y, z), \\ f_T^n(i, j, k, x, y, z) &= f(i, j, k) + \\ &\quad \sum_{l=1}^n \frac{1}{l!} \left((x - x_i) \frac{\partial}{\partial x} + (y - y_j) \frac{\partial}{\partial y} + (z - z_k) \frac{\partial}{\partial z} \right)^l \rho(x, y, z), \end{aligned} \quad (6)$$

where the derivatives have the meaning of numerical derivation of $f(i, j, k)$ from its grid values.

4. The 3D cubic interpolation:

$$\begin{aligned} \rho^C &= \sum_{i=1}^{ii} \sum_{j=1}^{jj} \sum_{k=1}^{kk} \sum_{l=1}^{nn} \sum_{m=1}^{nn} \sum_{n=1}^{nn} f_{lmn}^C(i, j, k), \\ \bar{\mu}^C &= \sum_{i=1}^{ii} \sum_{j=1}^{jj} \sum_{k=1}^{kk} \sum_{l=1}^{nn} \sum_{m=1}^{nn} \sum_{n=1}^{nn} \vec{r}_{lmn}(i, j, k) \cdot f_{lmn}^C(i, j, k), \\ f_{lmn}^C(i, j, k) &= \sum_{p=0}^3 \sum_{r=0}^3 \sum_{s=0}^3 w_{i,j,k}^{p,r,s} (x - x_i + l \cdot \Delta x / nn)^{(p)} \\ &\quad (y - y_j + m \cdot \Delta y / nn)^{(r)} (z - z_k + n \cdot \Delta z / nn)^{(s)}. \end{aligned} \quad (7)$$

In such approach each $\Delta x \times \Delta y \times \Delta z$ cell is divided into $(nn)^3$ subcells (nn in each direction) and the electron density is separately approximated by cubic 3D

polynomial in every subcell. In order to perform such approximation we have to assume that the first and second derivatives are continuous at the segment boundaries:

$$\begin{aligned}
 \rho_x^{(1)+}(x_0, y_0, z_0) &= \rho_x^{(1)-}(x_{ii}, y_{jj}, z_{kk}) & \rho_x^{(2)+}(x_0, y_0, z_0) &= \rho_x^{(2)-}(x_{ii}, y_{jj}, z_{kk}), \\
 \rho_y^{(1)+}(x_0, y_0, z_0) &= \rho_y^{(1)-}(x_{ii}, y_{jj}, z_{kk}) & \rho_y^{(2)+}(x_0, y_0, z_0) &= \rho_y^{(2)-}(x_{ii}, y_{jj}, z_{kk}), \\
 \rho_z^{(1)+}(x_0, y_0, z_0) &= \rho_z^{(1)-}(x_{ii}, y_{jj}, z_{kk}) & \rho_z^{(2)+}(x_0, y_0, z_0) &= \rho_z^{(2)-}(x_{ii}, y_{jj}, z_{kk}), \\
 \rho_x^{(1)-}(x_i, y_j, z_k) &= \rho_x^{(1)+}(x_i, y_j, z_k) & \rho_x^{(2)-}(x_i, y_j, z_k) &= \rho_x^{(2)+}(x_i, y_j, z_k), \\
 \rho_y^{(1)-}(x_i, y_j, z_k) &= \rho_y^{(1)+}(x_i, y_j, z_k) & \rho_y^{(2)-}(x_i, y_j, z_k) &= \rho_y^{(2)+}(x_i, y_j, z_k), \\
 \rho_z^{(1)-}(x_i, y_j, z_k) &= \rho_z^{(1)+}(x_i, y_j, z_k) & \rho_z^{(2)-}(x_i, y_j, z_k) &= \rho_z^{(2)+}(x_i, y_j, z_k),
 \end{aligned} \tag{8}$$

where $i = 1, \dots, ii - 1$; $j = 1, \dots, jj - 1$; $k = 1, \dots, kk - 1$.

Two different numerical expressions were used to calculate the first derivative. Method I uses the formula:

$$\frac{\partial}{\partial x} f^{\text{CI}}(i, j, k) = \frac{1}{2\Delta x} (f(i+1, j, k) - f(i-1, j, k)), \tag{9}$$

whereas method II calculates derivatives as:

$$\begin{aligned}
 \frac{\partial}{\partial x} f^{\text{CII}}(i, j, k) &= \frac{1}{8\Delta x} (f(i+1, j+1, k+1) - f(i-1, j+1, k+1) + \\
 & f(i+1, j+1, k-1) - f(i-1, j+1, k-1) + \\
 & f(i+1, j-1, k-1) - f(i-1, j-1, k-1) + \\
 & f(i+1, j-1, k+1) - f(i-1, j-1, k+1)).
 \end{aligned} \tag{10}$$

The corresponding expressions were used for the derivatives in other directions.

3. Results and discussion

As a test we calculated the dipole moment of simple molecules (*e.g.* H₂, H₂O, HB, CO, NH₃, PH₃, CH₄, C₁₀H₈). These molecules were placed inside a cubic supercell. The results for the total charge of considered electrons ρ [e] and the length of dipole moment μ [D] are given in Tables 1–9.

In all tables the following notation has been used: ()^D – the direct method, ()^I – the integration by parts method, ()^{T,1} – the Taylor expansion method, first order, ()^{T,4} – the Taylor expansion method, fourth order, ()^{CI,1} – the 3D cubic interpolation, method I, no subcells, ()^{CI,7} – the 3D cubic interpolation, method I, 7 subcells, μ^{Gast} – method of Gasteiger [7], ρ^{Exp} – number of electrons considered in calculated electron density, μ^{Exp} – experimental value of dipole moment [8].

Table 1. The total charge and dipole moment for H₂; the cubic supercell, side 5 Å, grid 30 × 30 × 30

| ρ^{D} | ρ^{I} | $\rho^{\text{T},1}$ | $\rho^{\text{T},4}$ | $\rho^{\text{CI},1}$ | $\rho^{\text{CI},7}$ | $\rho^{\text{CII},1}$ | $\rho^{\text{CII},7}$ | | ρ^{Exp} |
|-------------------|-------------------|---------------------|---------------------|----------------------|----------------------|-----------------------|-----------------------|---------------------|---------------------|
| 2.0 | 2.0 | 2.0 | 2.0 | 1.77 | 1.96 | 1.77 | 1.96 | | 2.0 |
| μ^{D} | μ^{I} | $\mu^{\text{T},1}$ | $\mu^{\text{T},4}$ | $\mu^{\text{CI},1}$ | $\mu^{\text{CI},7}$ | $\mu^{\text{CII},1}$ | $\mu^{\text{CII},7}$ | μ^{Gast} | μ^{Exp} |
| 0.01 | 0.0 | 0.02 | 0.02 | 0.05 | 0.01 | 0.05 | 0.01 | — | 0.0 |

Table 2. The total charge and dipole moment for H₂; the cubic supercell side 10 Å, grid 60 × 60 × 60

| | | | | | | | | | |
|----------|----------|--------------|--------------|---------------|---------------|----------------|----------------|--------------|--------------|
| ρ^D | ρ^I | $\rho^{T,1}$ | $\rho^{T,4}$ | $\rho^{CI,1}$ | $\rho^{CI,7}$ | $\rho^{CII,1}$ | $\rho^{CII,7}$ | | ρ^{Exp} |
| 2.0 | 2.0 | 2.0 | 2.0 | 2.34 | 2.04 | 2.34 | 2.04 | | 2.0 |
| μ^D | μ^I | $\mu^{T,1}$ | $\mu^{T,4}$ | $\mu^{CI,1}$ | $\mu^{CI,7}$ | $\mu^{CII,1}$ | $\mu^{CII,7}$ | μ^{Gast} | μ^{Exp} |
| 0.0 | 0.0 | 0.0 | 0.0 | 0.04 | 0.01 | 0.04 | 0.0 | 0.0 | 0.0 |

Table 3. The total charge and dipole moment for CH₄; the cubic supercell side 6 Å, grid 45 × 45 × 45

| | | | | | | | | | |
|----------|----------|--------------|--------------|---------------|---------------|----------------|----------------|--------------|--------------|
| ρ^D | ρ^I | $\rho^{T,1}$ | $\rho^{T,4}$ | $\rho^{CI,1}$ | $\rho^{CI,7}$ | $\rho^{CII,1}$ | $\rho^{CII,7}$ | | ρ^{Exp} |
| 8.0 | 8.0 | 8.0 | 8.0 | 8.17 | 8.02 | 8.17 | 8.02 | | 8.0 |
| μ^D | μ^I | $\mu^{T,1}$ | $\mu^{T,4}$ | $\mu^{CI,1}$ | $\mu^{CI,7}$ | $\mu^{CII,1}$ | $\mu^{CII,7}$ | μ^{Gast} | μ^{Exp} |
| 0.02 | 0.02 | 0.05 | 0.05 | 1.42 | 0.2 | 1.42 | 0.2 | 0.0 | 0.0 |

Table 4. The total charge and dipole moment for C₆H₆; the cubic supercell side 10 Å, grid 60 × 60 × 60

| | | | | | | | | | |
|----------|----------|--------------|--------------|---------------|---------------|----------------|----------------|--------------|--------------|
| ρ^D | ρ^I | $\rho^{T,1}$ | $\rho^{T,4}$ | $\rho^{CI,1}$ | $\rho^{CI,7}$ | $\rho^{CII,1}$ | $\rho^{CII,7}$ | | ρ^{Exp} |
| 30.0 | 30.0 | 30.0 | 30.0 | 30.99 | 30.15 | 30.99 | 30.15 | | 30.0 |
| μ^D | μ^I | $\mu^{T,1}$ | $\mu^{T,4}$ | $\mu^{CI,1}$ | $\mu^{CI,7}$ | $\mu^{CII,1}$ | $\mu^{CII,7}$ | μ^{Gast} | μ^{Exp} |
| 0.0 | 0.0 | 0.01 | 0.0 | 0.06 | 0.02 | 0.06 | 0.02 | 0.0 | 0.0 |

Table 5. The total charge and dipole moment for C₁₀H₈; the cubic supercell side 10 Å, grid 60 × 60 × 60

| | | | | | | | | | |
|----------|----------|--------------|--------------|---------------|---------------|----------------|----------------|--------------|--------------|
| ρ^D | ρ^I | $\rho^{T,1}$ | $\rho^{T,4}$ | $\rho^{CI,1}$ | $\rho^{CI,7}$ | $\rho^{CII,1}$ | $\rho^{CII,7}$ | | ρ^{Exp} |
| 48.0 | 48.0 | 48.0 | 48.0 | 50.16 | 48.34 | 50.16 | 48.34 | | 48.0 |
| μ^D | μ^I | $\mu^{T,1}$ | $\mu^{T,4}$ | $\mu^{CI,1}$ | $\mu^{CI,7}$ | $\mu^{CII,1}$ | $\mu^{CII,7}$ | μ^{Gast} | μ^{Exp} |
| 0.12 | 0.12 | 0.15 | 0.14 | 0.11 | 0.02 | 0.11 | 0.02 | 0.0 | 0.0 |

Table 6. The total charge and dipole moment for H₂O; the cubic supercell side 10 Å, grid 60 × 60 × 60

| | | | | | | | | | |
|----------|----------|--------------|--------------|---------------|---------------|----------------|----------------|--------------|--------------|
| ρ^D | ρ^I | $\rho^{T,1}$ | $\rho^{T,4}$ | $\rho^{CI,1}$ | $\rho^{CI,7}$ | $\rho^{CII,1}$ | $\rho^{CII,7}$ | | ρ^{Exp} |
| 8.0 | 8.0 | 8.0 | 8.0 | 9.07 | 8.16 | 9.07 | 8.16 | | 8.0 |
| μ^D | μ^I | $\mu^{T,1}$ | $\mu^{T,4}$ | $\mu^{CI,1}$ | $\mu^{CI,7}$ | $\mu^{CII,1}$ | $\mu^{CII,7}$ | μ^{Gast} | μ^{Exp} |
| 1.81 | 1.81 | 1.81 | 1.81 | 2.07 | 1.84 | 2.07 | 1.84 | 1.15 | 1.85 |

Table 7. The total charge and dipole moment for NH₃; the cubic supercell side 10 Å, grid 60 × 60 × 60

| | | | | | | | | | |
|----------|----------|--------------|--------------|---------------|---------------|----------------|----------------|--------------|--------------|
| ρ^D | ρ^I | $\rho^{T,1}$ | $\rho^{T,4}$ | $\rho^{CI,1}$ | $\rho^{CI,7}$ | $\rho^{CII,1}$ | $\rho^{CII,7}$ | | ρ^{Exp} |
| 8.0 | 8.0 | 8.0 | 8.0 | 8.59 | 8.09 | 8.59 | 8.09 | | 8.0 |
| μ^D | μ^I | $\mu^{T,1}$ | $\mu^{T,4}$ | $\mu^{CI,1}$ | $\mu^{CI,7}$ | $\mu^{CII,1}$ | $\mu^{CII,7}$ | μ^{Gast} | μ^{Exp} |
| 1.58 | 1.85 | 1.58 | 1.58 | 2.18 | 1.66 | 2.18 | 1.66 | 0.63 | 1.47 |

Table 8. The total charge and dipole moment for CO; the cubic supercell side 7 Å, grid 40 × 40 × 40

| ρ^D | ρ^I | $\rho^{T,1}$ | $\rho^{T,4}$ | $\rho^{CI,1}$ | $\rho^{CI,7}$ | $\rho^{CII,1}$ | $\rho^{CII,7}$ | | ρ^{Exp} |
|----------|----------|--------------|--------------|---------------|---------------|----------------|----------------|--------------|--------------|
| 10.0 | 10.0 | 10.0 | 10.0 | 10.97 | 10.14 | 10.97 | 10.14 | | 10.0 |
| μ^D | μ^I | $\mu^{T,1}$ | $\mu^{T,4}$ | $\mu^{CI,1}$ | $\mu^{CI,7}$ | $\mu^{CII,1}$ | $\mu^{CII,7}$ | μ^{Gast} | μ^{Exp} |
| 0.23 | 0.25 | 0.24 | 0.24 | 0.65 | 0.09 | 0.65 | 0.09 | — | 0.1 |

Table 9. The total charge and dipole moment for HF; the cubic supercell side 7 Å, grid 48 × 48 × 48

| ρ^D | ρ^I | $\rho^{T,1}$ | $\rho^{T,4}$ | $\rho^{CI,1}$ | $\rho^{CI,7}$ | $\rho^{CII,1}$ | $\rho^{CII,7}$ | | ρ^{Exp} |
|----------|----------|--------------|--------------|---------------|---------------|----------------|----------------|--------------|--------------|
| 8.0 | 8.0 | 8.0 | 8.0 | 8.28 | 8.05 | 8.28 | 8.05 | | 8.0 |
| μ^D | μ^I | $\mu^{T,1}$ | $\mu^{T,4}$ | $\mu^{CI,1}$ | $\mu^{CI,7}$ | $\mu^{CII,1}$ | $\mu^{CII,7}$ | μ^{Gast} | μ^{Exp} |
| 1.85 | 1.85 | 1.85 | 1.85 | 0.77 | 1.67 | 0.77 | 1.67 | 1.18 | 1.91 |

The first conclusion coming from these tables is trivial. If one likes to calculate the dipole moment one needs to have as accurate data on electron density as possible, which means that a large supercell is required and a fine grid should be used (*cf.* Tables 1 and 2). The comparison of the results shows that both the Taylor expansion method and the 3D cubic interpolation may modify the charge, so that it differs from the realistic one. The convergence to the realistic value requires a large number of terms in the expansion. The differences in the dipole moments calculated using various methods come from the fact that the electron density as a function of space is interpolated in different ways. For molecules with a small dipole moment the direct method and the integration by parts method as well as the Gasteiger procedure [7] give quite accurate results, whereas the Taylor expansion method and the 3D cubic interpolation are less accurate. However, for more interesting molecules with a large dipole moment, the last two methods seem to give more accurate results.

Using the techniques described above we may calculate the dipole moment of a hydrogen over TiH₂ (100) surface. We have considered an atom of H 1.768 Å over the top atom of titanium. Tables 10 and 11 show the charge and the dipole moment for a supercell with and without an extra atom.

As one can see the dispersion of results is large. The big difference between values obtained by methods 1–3 and 3D cubic interpolation arise from the fact that the electron density on the surface is a function which rapidly changes in space. If we subtract the results obtained using the same method, we can see that the presence of

Table 10. The total charge and dipole moment for cell TiH₂; the tetragonal supercell dimensions 5.46 × 5.46 × 20 Å, grid 32 × 32 × 120

| ρ^D | ρ^I | $\rho^{T,1}$ | $\rho^{T,4}$ | $\rho^{CI,1}$ | $\rho^{CI,7}$ | $\rho^{CII,1}$ | $\rho^{CII,7}$ | | ρ^{Exp} |
|----------|----------|--------------|--------------|---------------|---------------|----------------|----------------|--------------|--------------|
| 32.0 | 32.0 | 32.0 | 32.0 | — | — | 32.89 | 32.13 | | 32.0 |
| μ^D | μ^I | $\mu^{T,1}$ | $\mu^{T,4}$ | $\mu^{CI,1}$ | $\mu^{CI,7}$ | $\mu^{CII,1}$ | $\mu^{CII,7}$ | μ^{Gast} | μ^{Exp} |
| 19.27 | 19.26 | 18.82 | 18.82 | — | — | 0.99 | 0.31 | — | 0.0 |

Table 11. The total charge and dipole moment for H adsorbed on (100) TiH₂ 1.768 Å (top position); the tetragonal supercell dimensions 5.46 × 5.46 × 20 Å, grid 32 × 32 × 120

| | | | | | | | | | |
|----------|----------|--------------|--------------|---------------|---------------|---------------|---------------|--------------|--------------|
| ρ^D | ρ^I | $\rho^{T,1}$ | $\rho^{T,4}$ | $\rho^{CI,1}$ | $\rho^{CI,7}$ | $\rho^{CH,1}$ | $\rho^{CH,7}$ | | ρ^{Exp} |
| 33.0 | 33.0 | 33.0 | 33.0 | — | — | 34.15 | 33.17 | | 33.0 |
| μ^D | μ^I | $\mu^{T,1}$ | $\mu^{T,4}$ | $\mu^{CI,1}$ | $\mu^{CI,7}$ | $\mu^{CH,1}$ | $\mu^{CH,7}$ | μ^{Gast} | μ^{Exp} |
| 20.86 | 20.84 | 19.46 | 19.94 | — | — | 7.46 | 1.75 | — | — |

a single hydrogen atom changes the dipole moment by ~ 1 debye, however expected errors are much larger than this value.

4. The final remarks

Summarising, we would like to point out that although the DFT techniques are not most suitable for calculations of the electron density in the case of small molecules, nevertheless they may be directly used to estimate the dipole moment. We have found that custom written procedures, which interpolate the electron density data are usually more accurate than the Gasteiger's procedure supplied with the CASTEP program. However, in a more interesting case of an atom adsorbed on a metallic surface, such procedures are still not accurate enough to give a dipole moment of the adsorbed atom. In order to do it one needs to know the functional form of electron density in the whole system.

Acknowledgements

The authors are grateful to the Interdisciplinary Center for Mathematical and Computational Modelling, University of Warsaw, Poland (ICM UW) for a computational grant.

References

- [1] <http://www.accelrys.com/mstudio/castep.html>
- [2] 1997 *Cerius2 Quantum Mechanics*, Physics, CASTEP, ESOCs, FASTSTRUCTURE
- [3] Nowicka E and Duś R 1997 *Alloys J. and Compounds* **253–254** 506
- [4] Delchar T, Ebergahen A and Tomkins F C 1963 *J. Sci. Instrum.* **40** 105
- [5] Ross J, MacDonald and Barlow C A 1963 *J. Chem. Phys.* **39** 412
- [6] Lin J S, Qteish A, Payne M C and Heine V 1993 *Phys. Rev.* **B 47** 4174
- [7] Gasteiger J and Marsili M 1980 *Tetrahedron* **36** 3219
- [8] 1974 *Handbook of Physics and Chemistry*, collective work, WNT, Warsaw (in Polish)